Conformational Changes in the ApcT Amino Acid Transporter: Monte Carlo Normal Mode Following

Gennady V. Miloshevsky,[1] Ahmed Hassanein[1] and Peter C. Jordan[2]

[1]*School of Nuclear Engineering, Purdue University, West Lafayette, IN, USA*

[2]*Department of Chemistry, Brandeis University, Waltham, MA, USA*

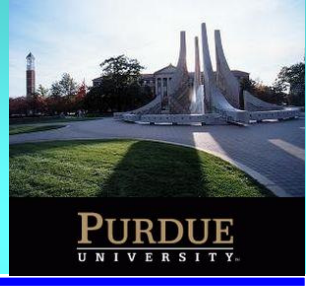

Abstract

Amino acid/polyamine/organocation (APC) transporters belong to a large family (~250) of secondary transport proteins that catalyze bilayer translocation of a broad range of substrates. Monte Carlo Normal Mode Following [1,2] is used to explore possible conformational change mechanisms in a proton-dependent APC transporter, ApcT, a bacterial homologue from *Methanocaldococcus jannaschii* [3]. ApcT was captured in an inward-facing apo state. Gating is initiated by global counter-torsions of the intracellular and extracellular domains of ApcT around the pore axis, with the extracellular half rotating clockwise and the intracellular half anticlockwise, and vice versa. The domain motions are highly concerted and cooperative. The stationary plane relative to which counter-torsion occurs passes through the center of ApcT parallel to the membrane. Extracellularly, overall rotation of the peripheral helices reconfigures TM6a significantly and TM1b slightly. These helices alternately approach and separate from the opposed peripheral TM10 and TM11, affecting the extracellular mouth. TM6a and TM1b move toward the protein's perimeter and become buried inside the protein. Loops and small helices on the intracellular surface of ApcT undergo large-scale rotations. Intracellular motion is similar. Overall peripheral helix rotation affects TM1a significantly and TM6b slightly, displacing them from and collapsing them onto TM8 and TM5. TM8 and TM5 alternately undergo large-scale bending near their midpoints. Starting normal mode following along the lowest-frequency eigenvector(s) describes early steps of the gating transition in the ApcT transporter.

Introduction

The majority of APC transport proteins appear to exhibit a uniform topology with twelve TM α-helical spanners in a single polypeptide, a prediction experimentally verified for ApcT [3]. The first five TM helices (TM1-TM5) are related to the second five helices (TM6-TM10) by a two-fold pseudo-symmetry axis running parallel to the membrane plane through the center of ApcT. The interface of these repeats forms the binding pocket for substrates. TM1 and TM6 are antiparallel to each other facing the binding site, and have breaks in their helical structure at midpoints.

It is suggested [3] that the mechanism by which ApcP effects the translocation of substrates involves cytoplasmic proton binding and unbinding to K158, modulating the conformation of TM1 and TM6 and thus facilitating the opening and closing of the extracellular and intracellular gates. However, atomic-level details of conformational changes associated with the full transport cycle are not known. Does isomerization between the inward-facing and outward-facing states of ApcT involve large-scale conformational reorganization spread throughout the protein backbone or does the substrate permeate through a sequence of dissociation-association steps along the pore without any significant effects on the backbone conformation? All-atom normal mode analysis (NMA) and mode following methods are used to probe the conformational changes in ApcT.

Computational Model

➢ We use the high-resolution (2.32 Å) X-ray structure of *Methanocaldococcus jannaschii* ApcT transporter (pdb entry 3GIA) [3] with 163 crystallographic waters. Protein hydrogens were added by using our MCICP code, creating 6,839 protein atoms. The overall molecular system contains a total of 7,328 atoms.

➢ The molecular system was described with the all-hydrogen CHARMM22 topology and parameter set, with NMA calculations carried out in vacuum.

➢ To remove steric clashes and to relax the molecular system, ~2,000 minimization steps were carried out using steepest descent with a random step length; finally, the molecular system was well tuned via conjugate gradient with guaranteed descent [4]. All degrees of freedom (bond lengths, bond angles, torsion and improper torsion angles) in the protein and waters were variable.

➢ The geometry of the molecular system with an absolute largest gradient component of $<5\cdot10^{-10}$ kcal mol^{-1} Å^{-1} was located. This extremely precise minimum is required when performing NMA on large protein structures where even small residual derivatives can lead to serious errors in the calculated eigendirections. Between crystal and minimized ApcT structures the RMSD for the C_α is 0.61 Å; that for all 7,328 atoms is 1.04 Å. These are small indicating that the minimized and crystal structures are highly similar.

➢ Standard all-mode NMA was carried out using the DSTEVR eigensolver from the LAPACK library and highly optimized BLAS routines for performing basic vector and matrix operations; global translational and rotational NMs were removed using the Eckart conditions. For the bonded and non-bonded energy terms both gradient and Hessian were calculated analytically; for other energy terms (angle, dihedral, improper and Urey-Bradley) a fourth-order finite-difference approximation was used.

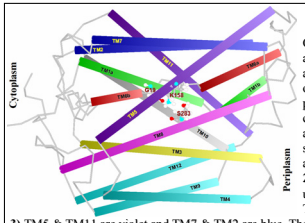

Minimized ApcT structure

Crystallographic waters are suppressed for clarity. K158, G19 and S283 are shown in the ApcT interior. The K158 (TM5) amine group forms H-bonds with the carbonyl and hydroxyl oxygens of G19 (TM1) and S283 (TM8); it is believed [3] to play an important role in gating. TM helices are represented as cylinders, with extracellular and intracellular ends shaded light and dark, respectively. TM helices are grouped as follows: **1)** "V-shaped" TM1 and TM6 are green and umber, respectively; they are broken at their midpoints and oriented relatively antiparallel. **2)** TM3 is yellow, TM8 is pink and TM10 is grey. These abut the unwound parts of TM1 and TM6. The inner helices, TM1, TM6, TM3, TM8 and TM10 form the substrate transport pore. **3)** TM5 & TM11 are violet and TM7 & TM2 are blue. These perimeter helices surround TM1 and TM6. **4)** TM4, TM9 and TM12 are cyan, comprising another set of perimeter helices surrounding the inner TM3, TM8 and TM10. The figure was generated using our MCICP code.

Eigenvalues of the minimized ApcT systems

Three ApcT systems with charged K158 (denoted K158$^+$ ApcT) and the two ApcT systems with neutralized K158 (denoted K158^n ApcT) were minimized and NMs calculated

➢ for all five ApcT systems the first six eigenvalues are near zero and other eigenvalues are positive indicating a minimum

➢ one set of eigenvalues for charged K158$^+$ ApcT and one for neutralized K158^n ApcT are shown on the left- and right-hand side respectively. The lowest-frequency eigenvalue (7th) was close in all three K158$^+$ ApcT systems: 3.49, 3.96 and 3.79 cm^{-1}, respectively. This eigenvalue is 3.78 and 4.26 cm^{-1} for the two K158^n ApcT systems

➢ the lowest-frequency eigendirections are nearly identical for all five ApcT systems, with overlaps of ~1

Main observation: neutralizing K158 at the binding site in the ApcT transporter has no effect on the lowest-frequency normal mode

K158$^+$ ApcT	
n	ν, cm^{-1}
1	-3.46E-05
2	-1.89E-05
3	-1.09E-05
4	1.89E-05
5	2.45E-05
6	4.73E-05
7	3.48771
8	4.09168
9	5.00522
10	5.05008
11	5.67546
12	6.05163
...	.....

K158^n ApcT	
n	ν, cm^{-1}
1	-2.09E-05
2	-6.32E-06
3	1.89E-05
4	2.45E-05
5	3.84E-05
6	4.00E-05
7	3.77967
8	4.48925
9	5.14761
10	5.81197
11	6.41629
12	6.70530
...	.....

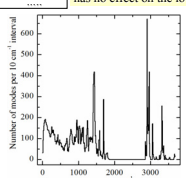

Frequency Spectrum of the K158$^+$ ApcT System

- the frequency spectrum is the same in all five runs
- the region < 590 cm^{-1} describes concerted motions of secondary structure elements (α-helices and large groups of amino acids)
- the region from 590 to 1840 cm^{-1} corresponds to internal vibrations of single amino acids
- the region > 2850 cm^{-1} corresponds to hydrogen-heavy atom vibrations

7-th Normal Mode of the K158$^+$ ApcT system

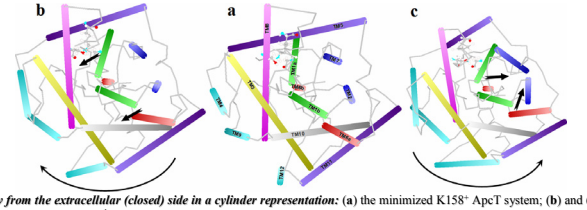

View from the extracellular (closed) side in a cylinder representation: (**a**) the minimized K158$^+$ ApcT system; (**b**) and (**c**) displacement along the 7th all-atom NM in the "plus" and "minus" directions.

- Overall highly concerted and cooperative counter-rotations (black curved arrows) of the intracellular and extracellular domains around the pore axis. In counter-rotation the extracellular half of ApcT rotates clockwise, while the intracellular half rotates anticlockwise, and vice versa. The stationary plane relative to which the rotation occurs passes through the center of ApcT parallel to the membrane.
- Both extracellularly and intracellularly, overall rotation of the peripheral helices reconfigures the inner helices (TM1, TM6, TM3, TM8 and TM10). The V-shaped TM1 (green) and TM6 (red) helices alternately straighten and bend at their midpoint breaks (black straight arrows). Side chain of K158 undergoes large-scale displacement and rotation (~150^0) around its own chain axis. Loops and small helices on both sides undergo large-scale rotational motion.

8-th Normal Mode of the K158$^+$ ApcT system

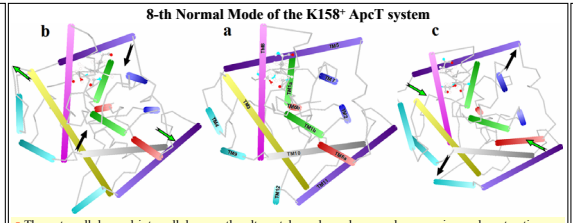

- The extracellular and intracellular mouths alternately undergo large-scale expansion and contraction: as the extracellular mouth expands, the intracellular mouth contracts and vise versa. The extracellular ends of the peripheral TM5 (light violet) and TM7 (light blue) approach and separate from the diagonally opposed peripheral TM9 (light cyan) and TM10 (light grey) (black arrows). Alternatively, the intracellular ends of TM4 (dark cyan) and TM5 (dark violet) approach and separate from the diagonally opposed TM10 (dark grey) and TM11 (dark violet) (green arrows). This motion affects the inner TM1 (green) and TM6 (red) (V-shape) on both sides displacing them off and collapsing them on the inner TM10 (grey) and TM8 (pink). Side chain of K158 again undergoes displacement and large-scale rotation around its own chain axis.

9-th Normal Mode of the K158$^+$ ApcT system

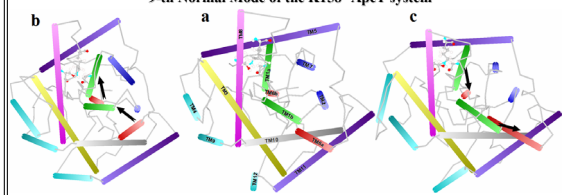

- The extracellular and intracellular ends of TM1 (green) and TM6 (red) bend/twist in unison and concertedly at their midpoint breaks (black straight arrows). This motion has no significant effect (although there is significant lateral bending) on the V-shape of TM1-TM6.

Conformational Changes at the Site of the K158 Side Chain

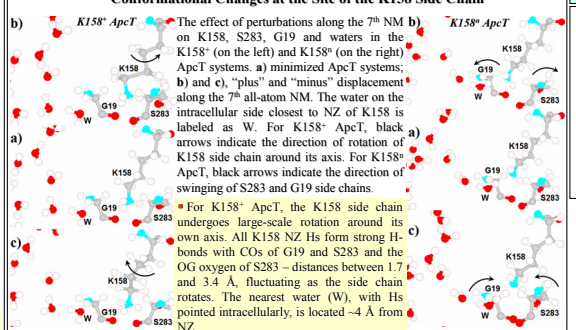

The effect of perturbations along the 7th NM on K158, S283, G19 and waters in the K158$^+$ (on the left) and K158^n (on the right) ApcT systems. **a**) minimized ApcT systems; **b**) and **c**), "plus" and "minus" displacement along the 7th all-atom NM. The water on the intracellular side closest to NZ of K158 is labeled as W. For K158$^+$ ApcT, black arrows indicate the direction of rotation of K158 side chain around its axis. For K158^n ApcT, black arrows indicate the direction of swinging of S283 and G19 side chains.

- For K158$^+$ ApcT, the K158 side chain undergoes large-scale rotation around its own axis. All K158 NZ Hs form strong H-bonds with COs of G19 and S283 and the OG oxygen of S283 – distances between 1.7 and 3.4 Å, fluctuating as the side chain rotates. The nearest water (W), with Hs pointed intracellularly, is located ~4 Å from NZ.
- For K158^n ApcT, K158 side chain motion changes crucially. It swings with insignificant rotation around its own axis. The G19 and S283 side chains alternately approach and separate from NZ of K158. Water W forms an H-bond with NZ (distance <2 Å) and is also connected to an intracellular water chain. We speculate that the proton can directly access NZ of K158 along this continuous water chain. The side chain of S283 with its OG screened by the NZ group of K158 is not accessible to the intracellular water. Thus, protonating/deprotonating K158 influences the character of the local motion of K158 and nearby residues.

Pore Size of K158$^+$ ApcT Perturbed along the 7th NM

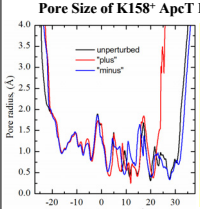

Main observations:

➢ In perturbing to an RMSD of 3.5 Å along the 7th NM in either direction, the extracellular pore (from 0 to 20 Å) stays closed, fluctuating slightly in size. The intracellular pore (from -20 to 0 Å) remains nearly unchanged and is constricted, with a radius <~1 Å.

➢ The protein's extracellular mouth (from 20 to 30 Å) opens ("plus" direction) wide. The intracellular mouth (< -20 Å) is nearly unaffected.

Tracking the K158$^+$ ApcT system using all-atom MC-NMF

This work is in progress. Our parallel MCICP code runs on the Purdue TeraGrid system (Steele Dell Intel 64 Linux Cluster), but more optimization is needed. The lowest frequency eigenvector of the K158$^+$ ApcT system has been tracked for 30 MC steps using the all-atom MC-NMF technique [1,2]. Gating onset follows the 7th NM. However, local side chain reorganizations proceeding global backbone motions are also seen. Water molecules move as integral structural elements.

Conclusions

- All-atom NMA identifies the intrinsic directionality of conformational changes in the ApcT backbone for initiating a gating transition. The large-scale motions of the protein backbone along the first two low-frequency NMs affect the V-shape conformation of the inner TM1 and TM6 helices; they alternately straighten and bend at their midpoint breaks. Unlike LeuT$_{Aa}$ [5], conformational changes in ApcT are highly alike on the extracellular (closed) and intracellular (open) sides.
- The K158 side chain, located near intracellular waters (~3-4 Å), undergoes motion and large-scale rotation around its chain axis, suggesting that this residue can be involved in proton transport [3]. Upon deprotonation of its NZ atom, the nature of the motion changes from rotation around its axis to swinging in the plane perpendicular to the membrane. The reason for this change remains to be investigated. In the K158^n ApcT system, a continuous water chain is formed connecting NZ of K158 to the intracellular solution. We speculate that a proton can shuttle along this water wire.

References

1. Miloshevsky & Jordan, *Structure* **14**, 1241 (2006)
2. Miloshevsky & Jordan, *Structure* **15**, 1654 (2007)
3. Shaffer *et al.*, *Science* **325**, 1010 (2009)
4. Hager & Zhang, *SIAM J. Optim.* **16**, 170 (2005)
5. Miloshevsky & Jordan, *Biophys. J.* **94**, 740a (2008)

Acknowledgement

Work supported by a grant from the National Institutes of Health, GM-28643 and Purdue University. Computational resources provided by the NCSA under grant MCB080096N.